31st Congress of the International Council of the Aeronautical Sciences

Belo Horizonte, Brazil; September 09-14, 2018

LOCAL MODEL NETWORKS APPLIED TO FLIGHT LOADS ESTIMATION

Martin Halle* , **Frank Thielecke***

***Hamburg University of Technology, Hamburg, Germany**

Keywords: *maneuver,flight,loads,estimation,LMN*

Abstract

Nowadays flight load exceedance monitoring is an important task to the aircraft manufacturer as well as the operator. The estimation of flight loads is required during development and operation of an aircraft. The requirements are usually different for e.g. calculation of design loads for certification and operational loads monitoring of stress and fatigue. The ability to (more) precisely determine aircraft operational loads may reduce the time for analysing incidents and maintenance.

In this paper the system identification method of Local Model Networks is applied to the field of flight loads estimation for the use in offline-analysis but also for on-board aircraft systems by means of a data recorder storing direct loads indicators like forces and moments from estimates. The application of a previously developed modelling approach for flight loads estimation based on design and flight test data is used to model the loads acting on the horizontal tail plane of an aircraft.

1 Introduction

Structural hidden cracks due to maneuvers or fatigue can lead to critical situations as for example in the case of Air Transat, flight number 961 [1] or even loss of the aircraft. As shown in [1], inspection procedures maybe inadequate and therefore, fatigue effects in the structure are not detected. A committee of the Aerospace Industries Association (AIA) and the Air Transport Association (ATA) evaluated existing special inspection procedures for high load events like severe turbulence encounter or extreme maneuvering [2]. Instructions for such events are typically specified in aircraft maintenance manuals and are typically referred to as “Unscheduled Maintenance” or “Special Inspections”. The safety recommendations by the National Transportation Safety Board (NTSB) address a better detection of aircraft damage following an in-service (high load) event before returning the aircraft to service. They suggest areas where improvements can be implemented, for example to “the introduction of additional objective criteria using flight data to assist in the evaluation of events” and “the development of refined algorithms by the manufacturer that use multiple data parameters to arrive at improved evaluations of the severity of the loads actually experienced, and corresponding required actions”.

An estimation of the loads acting on the aircraft during normal and abnormal operation is necessary. Resources are generally restricted on-board an aircraft, therefore, efficient algorithms with a small resource footprint such as the ones presented in this publication are desired.

Targeting on-board systems several *indirect methods* with their own advantages and disadvantages exist. Existing methods presented in the first section of this paper show a respectable performance. Previous studies [4] introduce the approach of LMNs to estimate loads on the vertical tail plane (VTP) of an aircraft. Within this publication, the concept of LMNs will be improved and applied to estimate load quantities on the horizontal tail plane (HTP) of an aircraft, focusing

on events where high flight loads occur.

Following an introduction to LMNs, a section provides the problem definition with respect to HTP loads. After that, the data selection and the training process to obtain the models for the HTP are explained. Similar to [4] the *2-step-approach* to obtain the models is explained and presented.

The modelling (training-) process to obtain the models to estimate flight loads on the HTP is explained in detail. The LMN approach is enhanced to cope with the characteristic of the training data. A-priori knowledge is applied to achieve better results. The derived models for flight load estimation are presented. The results are quantified with respect to the aircraft's limit loads and the estimation quality achieved using the proposed method is presented.

A summary concludes the results and provides an outlook for future application of the methodology in further scenarios.

2 Existing Methods

In general, flight loads can be measured directly by instrumenting an aircraft with strain gauges [6], fibre Bragg grating sensors [7], [8] or piezoelectric sensors [9] at points of the aircraft structure where a measurement is desired. Such instrumentation can be found on test aircraft but is not available on standard aircraft due to weight, maintenance effort and costs. Therefore, typically indirect approaches are used instead.

Very often, due to their lightweight character, artificial neural networks (ANN) are being utilised to estimate flight loads based on models. Examples for different types of aircraft have been investigated in [10], [11], [12], [13], [14] or [15]. Further overviews of methodologies in the field of loads monitoring are also presented in [5].

In [3] and [4] it was shown that compared to ANN, LMNs are more robust due to their local linear approximation and a controllable extrapolation behaviour. It was summarised that LMNs clearly outperform neural networks. Load estimators for different target loads at structural parts of an aircraft have been developed. Within this paper LMNs are used again and have been further improved for the use-case of flight loads estimation.

3 Local Model Networks

The *Local Model Network* (LMN) approach has been described by [16], [17], [20], [5] and others. The modelling approach is based on measurement data used to create the models through a "training phase". During the training, the input space is decomposed to allow a specific modelling of different regions in the input space, referred to as *subspaces*, *local models* or *submodels*. The models are obtained in an iterative, self-organising process to cluster the input space.

For clustering the input space, different clustering algorithms exist [18], [19], [21]. In this paper, an axis-orthogonal decomposition of the input space is used. The local models are represented by rectangular partitions along the axis of the input space. In the case of high dimensionality these are hyper-rectangles. The behaviour of the system is modelled locally by considering only the training-data samples which lie within a specific hyper-rectangle that defines a subspace of the overall input space.

For a specific subspace i out of m subspaces, a locally linear function is determined by a linear, multivariate least squares approximation. The vector of regression coefficients $\mathbf{w}$ is determined by a least squares approach from the matrix of input parameters $\mathbf{U}$ and the vector of output parameters $\mathbf{y}$, both obtained from the measurement data:

$$\mathbf{w} = (\mathbf{U}\mathbf{U}^T)^{-1}\mathbf{U}^T\mathbf{y} \; . \tag{1}$$

For a system of k dimensions and an input vector $\mathbf{u}$, the linear approximation function y_i for the subspace i is

$$y_i(\mathbf{u}) = w_0 + \sum_{j=1}^{k} w_j \cdot u_j \; . \tag{2}$$

Due to the linear approximation, the locally determined function y_i which is valid for a certain segment $\left[a_{i,j}..b_{i,j}\right]$ of the input space will extrapolate for input data beyond the subspace used to determine the function. The activity of the linear

function (or local model of a subspace) is controlled by a *weighting-function* which is defined by normalised Gaussian for each dimension. The center c of each Gaussian function lies in the center of the segment. The standard deviation of the Gaussian is chosen to cover the range of the subspace in the respective dimension, while asymptotically becoming Zero outside of the subspace. For an input $\mathbf{u}$ of a system, the combined activity of all Gaussian functions for the current model i is determined by the local activation μ_i as

$$\mu_i(\mathbf{u}) = \exp\left(-\frac{1}{2}\sum_{j=1}^{k}\left(\frac{u_j - c_{i,j}}{\sigma_{i,j}}\right)^2\right), \quad (3)$$

with $c_{i,j} = \frac{a_{i,j}+b_{i,j}}{2}$ and $\sigma_{i,j} = \frac{2}{5}\left(b_{i,j} - a_{i,j}\right)s$ as proposed in [20]. The factor s is called *smoothness factor* and can be chosen during modelling to control the width of the Gaussian. This reflects the influence of one local model to its neighbours in the input space. The normalised weighting-function Φ_i is determined as

$$\Phi_i(\mathbf{u}) = \frac{\mu_i(\mathbf{u})}{\sum_{j=1}^{m}\mu_j(\mathbf{u})}. \quad (4)$$

The equation for the overall local model *network* follows to

$$\hat{y}(\mathbf{u}) = \sum_{i=1}^{m}\left(\Phi_i(\mathbf{u})[w_{i,0} + \sum_{j=1}^{k} w_{i,j}\cdot u_{i,j}]\right). \quad (5)$$

The structure of the resulting model is depicted in figure 1. Due to the overlapping character of the Gaussian functions, the predictions made by the different locally accurate models are superimposed in boundary regions leading to a steady transition between adjacent local models.

The input space decomposition is an iterative process leading to a steadily increased accuracy of the LMN. The decomposition is based on an initial global model by bisecting the input space orthogonally to each input dimension, resulting in at least two new local models per input dimension. The bisection, or "split" is chosen either by a-priori knowledge or (default case) such that the largest reduction in the global prediction error is achieved. The decomposition stops at either a certain prediction error or a certain maximum number of local models. Due to the transparent model structure and local linear functions, the structure also allows for physical interpretation and specific adaptation.

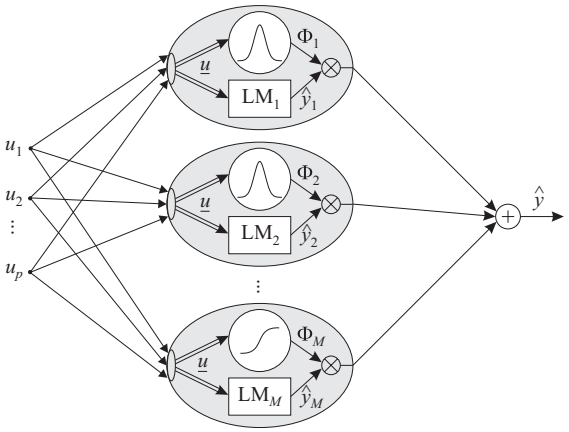

Fig. 1 Structure of a Local Model Network

4 Problem Definition

In [4], the structural flight maneuver loads of a vertical tail plane (VTP) of a transport aircraft have been modelled using the LMN approach. In this paper, the loads at the horizontal tail plane (HTP) are modelled using the same approach. The flight loads considered hereby are the bending moment M_x, the torsional moment M_z and the shear force F_z (see figure 2). Only aircraft system parameters available through a standard aircraft instrumentation (measurement platform) shall be used without any additional sensors. For the loads, special attention is drawn to high load occurrences.

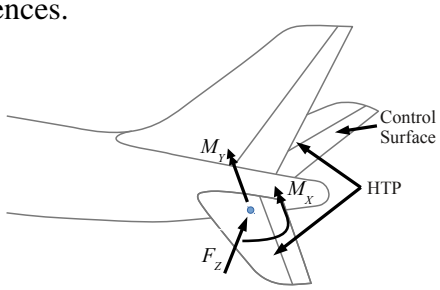

Fig. 2 Load components at the root of a HTP

External loads caused by the interaction of the aircraft with the environment result in maneuver loads acting on the structure of the aircraft.

Maneuver loads are classified into *steady loads* as in steady flight conditions and *incremental loads*, induced by maneuvers or inhomogeneous flow conditions as these are caused by gusts. At any position of the structure the local structural load F_{loc} during flight is the result of the superimposed external loads, namely aerodynamic loads F_{Aero}, propulsional loads F_{Prop}, inertial loads F_{Inert} and gravitational loads F_{Grav}:

$$F_{loc} = f(F_{Aero} + F_{Prop} + F_{Inert} + F_{Grav}) \,. \quad (6)$$

In this paper, internal structural loads shall be determined, assuming knowledge of the external loads. The desired models are a mathematical representation of a mapping function between the measured signals and the loads, such that they represent the aircrafts behaviour by means of the occurring external loads. This mathematical formulation is derived by applying the LMN approach and has been introduced more thoroughly in [3] and [4]. In contrast to direct loads measurement sensors, these models are "*virtual loads sensors*".

4.1 Data selection

For all data-driven modelling approaches and especially for methods using training data like LMNs, the selection of the data for training and validation is vital to achieve a desired model accuracy. Ideally, the input range should be evenly sampled. The LMNs will interpolate or extrapolate in regions, where less or no data is available. This can cause problems, shown and discussed in [3]. However, flight test data is usually not distributed homogeneously across the input space at all, therefore, special attention has to be paid to prepare good training data.

A database containing the aircraft system parameters from a specific transport aircraft is used as in [4]. This database was gathered through structural design calculations based on computer simulations and in different flight test campaigns. It covers about 4400 of so-called "load cases" of design calculations [22]. The maneuvers of the design calculations are grouped and represent a good coverage of the complete speed/altitude range of the aircraft. Such data is usually available even before the aircraft exists [22]. In contrast to that, there is also about 6 hours of flight test data for different flight conditions available, but only within a safe flight envelope [23]. Therefore, the flight test data covers a much smaller range, due to the safe flight envelope the aircraft has to be operated in.

The advantage of design calculations over flight test data is not only its complete flight envelope, they also account for extreme load cases. In real flight tests, flight loads are usually below 80% limit load. To cope with such, in [4] a *2-step-approach* has been proposed that is used again for modelling the HTP loads. In the first step, data from design calculations including high loads is used to create and train the models with focus on high loads. In a second step, flight test data is used to refine the models.

Additionally, as in [4], correlated 2D load envelopes for combined loads are taken into account, because the occurrence of load combinations can stress structural components significantly more. The 2D load envelopes are available throughout the aircraft structural design and describe the relation between two load components such as torsional (M_Y) and bending moment (M_X) by means of the maximum allowable loads.

For each of the 4400 design calculations the data samples with the highest loads are kept in the training data for both load components to ensure that the training data covers the areas with highest loads for each maneuver. To focus on high loads, the remaining data below a certain limit load threshold is reduced by re-sampling.

The resulting database is divided into training data where round-about 80% of the database is used. The remaining 20% are added to the validation data.

The data selection is done iteratively based on the insights gained from the model making use of its transparent character. For example: As explained previously, LMNs are a compound of local linear models with a Gaussian function defining the activity of the linear model. Figure 3 shows the simulation results for one of the independent validation data sets (maneuvers). The

reference values are in the upper part and the influence of the most dominant local models based on their weighting functions are in the lower part.

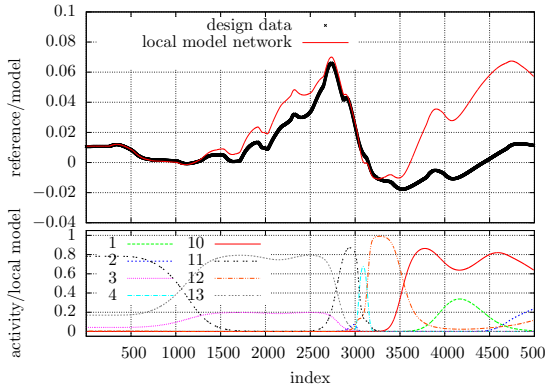

Fig. 3 Model weights with respect to model deficits

A large bias is observed starting at index 3500 that obviously corresponds to the local model no. 10. In the particular local model (subspace) are too few samples and lead to a large interpolation region. Providing more data within this subspace reduces the bias significantly as shown in figure 4.

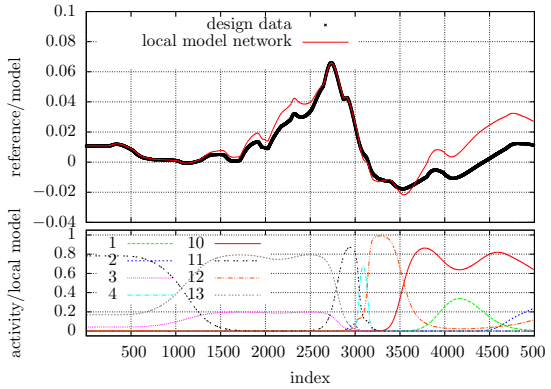

Fig. 4 Improved model after updating the database for training

Similar phenomena could also be the result of an extrapolation. Again, this approach provides very good insight into the distribution of the data in such particular subspaces. In [5] it is explained, how providing additional data or controlling the clustering algorithm leads to significant improvements and numerical stable local models.

4.2 Parameter selection

To find a model for the estimation of loads by means of a mapping function the following lists the parameters, which describe the state of the aircraft sufficiently with respect to the considered target loads on the HTP and is based on the approach as presented in [3] and [4].

Table 1 shows the parameters chosen for each of the considered load components.

Description	Symbol
Angle of attack	α
Sideslip angle	β
Horizontal stabiliser setting	δ_i
Elevator deflection	δ_q
Longitudinal load factor (LF)	N_x
Lateral LF	N_y
Vertical LF times aircraft mass	$N_z \cdot W$
Aircraft mass	W
Roll rate	p
Roll acceleration	$\dot{p}$
Pitch rate	q
Pitch acceleration	$\dot{q}$
Yaw rate	r
Dynamic pressure	q_{dyn}

Table 1 Selected parameters to model HTP loads

It has been observed, that the most sensitive parameters are angle of attack α, elevator deflection δ_q, horizontal stabiliser setting δ_i, dynamic pressure q_{dyn} and vertical load factor N_z. The vertical load factor N_z is used in combination (multiplied) with the aircrafts mass W, giving a vertical force ($F_z = N_z \cdot W$). In contrast to [4], making use of the dynamic pressure q_{dyn} instead of the true airspeed V_{TAS} leads to improved results.

The estimation for the sub-models of the LMN is based on linear functions. The input parameters are chosen whenever possible in a way, that they correlate highly linear with the target load (see an example for N_z wrt M_x in the upper part of figure 5). However, some parameters like the δ_i show no linear dependency and (even worse) as the trimming of the horizontal stabiliser is not continuously they have a partially

"discrete" character, shown in the lower part of figure 5.

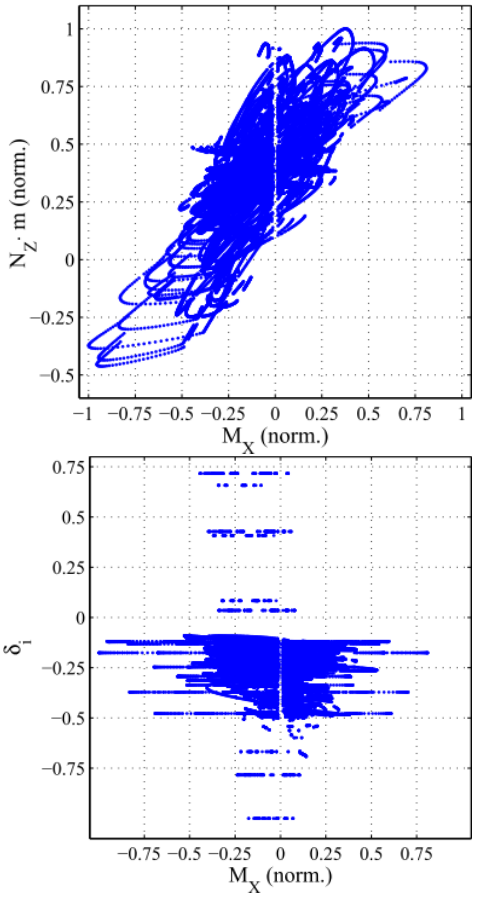

Fig. 5 Correlation between vertical load factor in contrast to horizontal stabiliser setting wrt bending moment

For LMNs, the clustering algorithm often stops at such conditions, as subspaces do not contain sufficient samples or the samples are not well (equally) distributed.

5 Results

In this section, the result of the modelling using the *2-step-approach* for the selected target loads is presented. For modelling, an in-house software framework named SIGMA that implements the modelling-, analysis and visualisation techniques is used. The LMN approach provides only a few parameters to adjust, explained in the following:

1. The *splitting ratio* defines how many splits of the subspaces in each iteration step are evaluated. A ratio of 1:1 splits a subspace exactly in the middle resulting in two equally sized new local models. A ratio of 1:2 results in actually 2 splits being evaluated with 1/3 to 2/3 and 2/3 to 1/3 respectively. Consequently, the split with minimal error of the cost function is chosen. In this study a ratio of 1:3 has been used.

2. The *smoothness factor* controls the overlapping effect of local models. In this study a smoothness factor of 0.9 has been selected.

3. The *maximum number of models* is the termination criteria to stop the training. In this study it has been set to 15.

The splitting algorithm from the literature [17] has been improved to cope with partial discrete input signals as mentioned in the previous chapter. In the case that the default splitting ratio leads to subspaces without samples and would stop, the borders of the subspace are temporarily being moved towards the data samples to continue instead, as illustrated in figure 6.

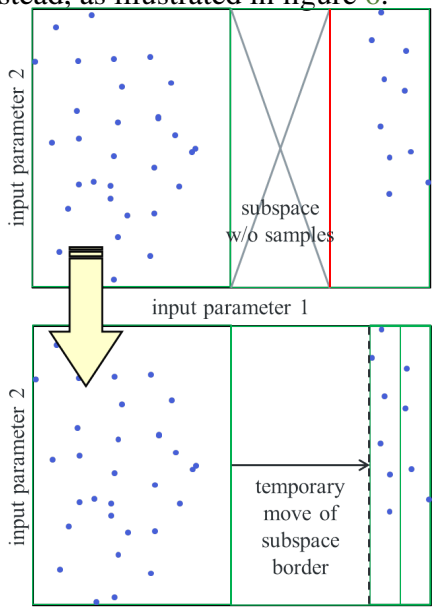

Fig. 6 Optimised splitting algorithm

In the upper part of the figure in the right subspace, a split in the dimension of the first input parameter is not possible (assuming a ratio of 1:1). In that case the splitting algorithm will

temporarily move the left border of the right submodel to allow the splitting algorithm to work. The drawback of this heuristic is that the splitting ratio is not equivalent across the input space.

For the assessment, the target values (loads) are normalised to 100% limit load, a load of 1 denotes 100% limit load. To visualise the results with respect to a 2D load envelope, the *2D criteria* from [4] is used to assess the models with respect to the combined loads. It is based on the *radial coefficient* where each correlated load condition is determined by two load components $C1$ and $C2$ provided by the respective load envelopes. Such load condition can be defined by an angle φ and the absolute value of its distance to the origin of the load envelope. The *radial coefficient* is the ratio of the load condition and the limit load at this angle as

$$\mathrm{RC} = \frac{\sqrt{C1^2 + C2^2}}{E(\varphi)} \quad . \tag{7}$$

The value of $RC \leq 1$ represents loads lower than limit load and $RC > 1$ when limit load is exceeded. These values are plotted for the model and reference in a correlation graph that visualises the quality of the estimation with respect to both load components.

For the pair of torsional moment M_y and shear force F_z, LMNs have been developed – one LMN for each load component. They generalise well on the design data as shown in the upper part of figure 7 that shows the result for the validation data set based on data of the design calculations for a certain modelling step.

The dotted lines mark a tolerance range of 10 and 20% estimation error. For high loads no major outliers are observed, most values are within the tolerance range of 10%. For lower loads there are outliers in the red circle that are outside of the 20% tolerance range.

The data corresponds to a "smooth push-over" maneuver that is obviously underrepresented. Better results with new training data gained from this type of maneuver are shown in the lower part of figure 7. Here, for the same set of validation data, the outliers are reduced.

The results presented so far are based on data from design calculations. In the second step of

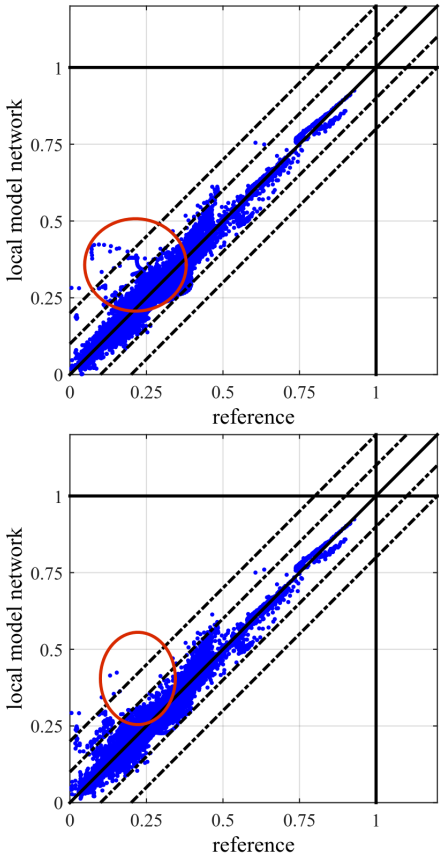

Fig. 7 RC correlation plot for non- and optimised set of training data wrt M_y and F_z

the *2-step-approach* the models are applied to flight test data and similar results are observed as presented in [4]: The models "as-is" show the right characteristic, but also some deficits. As an example for such, a special HTP maneuver of type "checked maneuver" is shown in the time domain with respect to the torsional moment M_y. During this maneuver the aircraft moves horizontally and different amplitudes to the elevator are commanded causing high torsional moments on the HTP. As shown in the upper part of figure 8, the simulation results have the right shape, but they are also biased.

Although the error is quite low and within a 6% margin, such deficit is addressed. The bias is a result of a LMN operating in an extrapolation area. That means, that at least one input parameter of the flight test data is outside the boundaries of the LMN. In this case, it is the longitudinal load factor N_x which is 30% above the maximum

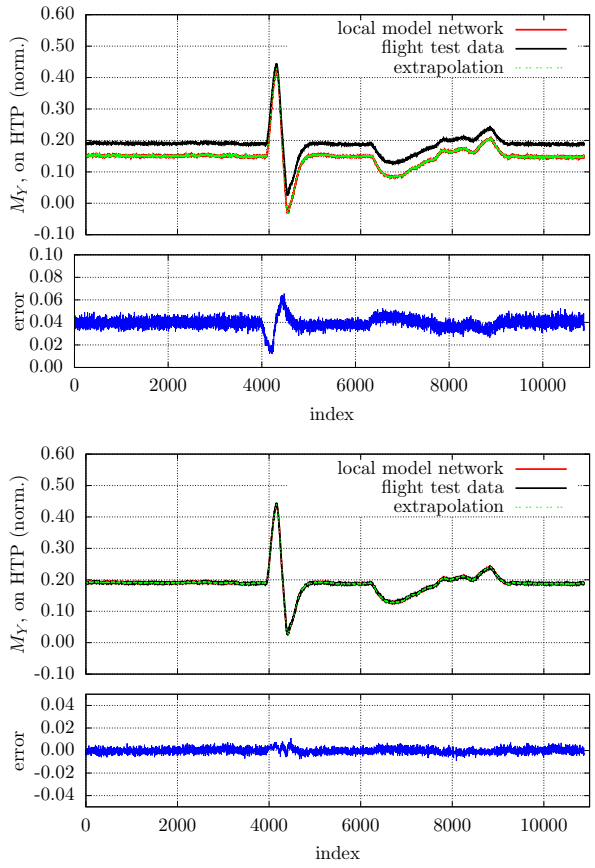

Fig. 8 Maneuver simulation with flight test data for interim and improved model

of the training data.

The extrapolation behaviour of LMNs is controllable and defined through an "extrapolation strategy". For this study, the extrapolation strategy to limit the input parameter to the border of the respective sub-model is sub-optimal.

A good solution would be to extend the data base using design calculation for larger N_x. Unfortunately, within this study this was not possible. Alternatively the extrapolation strategy could be changed. Within this study, the training data base is extended by using flight test data of that region, again similar to [4]. Then, the existing LMN is being re-trained using that data. While in [4] the structure of the LMN has been kept fixed, in this study an improved training algorithm capable to extend the borders of an existing LMN upon new data was used. Thus, all parameters of the local models are re-estimated after extending the borders of the respective sub-models. The result for the updated model with respect to the maneuver from above is shown in the lower part of figure 8.

The bias and therefore, the error for this maneuver is greatly reduced. However, this is only valid for the selected, single maneuver. To compare the overall performance the correlation between the LMN and the flight test data with respect to combined loads of torsional and bending moment M_Y/M_X and based on the 2D criteria is analysed.

By means of the RC correlation plot, figure 9 shows the results for the validation data based on the complete flight test data before and after the parameter- and structure update. Again, two dotted lines mark an estimation error of 10 and 20% respectively.

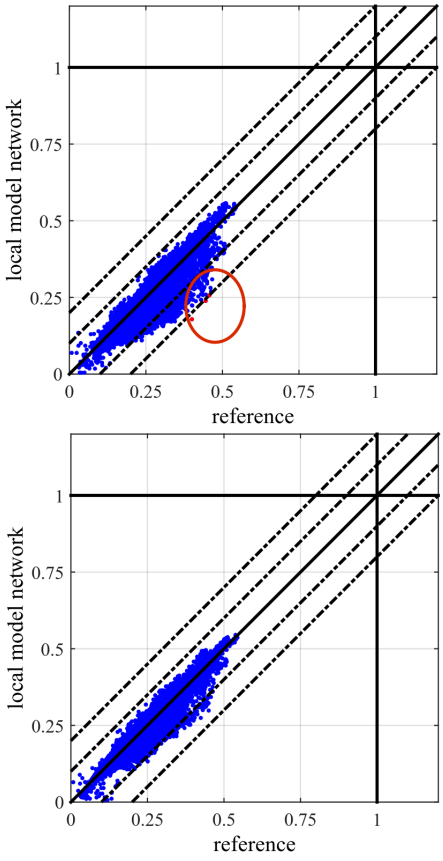

Fig. 9 RC correlation plot of original and updated LMN wrt F/T data

In the upper plot, the area with major outliers for the flight test data is depicted with a red circle. After the model update (in the lower plot) the error margin is nearly 10% and well improved. It

can also be seen, that flight test data is usually well below 80% limit load. In the case of the flight test data that was available for the HTP it was even smaller, only slightly above 50% limit load. Similar results were achieved for the combination of torsional moment and shear force.

6 Summary

Monitoring of specific component loads of aircraft structures is desired without the need for additional sensors. Models to estimate loads based on indirect methods known from the literature use flight parameters that are available with the standard-instrumentation of an aircraft and provide non-measurable target loads.

In [3] a new data-based approach based on local model networks (LMNs) has been presented to estimate flight loads targeting on-board aircraft systems. This system identification method is compared to neural networks (ANN) and shows major advantages over existing ANN approaches with respect to a more robust inter- and extrapolation behaviour.

In [4] the same approach has been further improved by introducing a so-called *2-step approach* for the modelling. The models are initialised based on data from structural design calculations and then refined and optimised based on data from flight tests. The approach has been successfully applied to model the structural loads on a vertical tail plane (VTP) of an aircraft.

Within this study, the approach is now applied to model the structural loads on a horizontal tail plane (HTP) of an aircraft. This component shows a different characteristic compared to the VTP. Similar to [4] the data base used for the training and validation of the models is obtained in an iterative process. Tools to gain insights into weak spots of the model structure provide the capability to resolve model deficits by making use of system- and a-priori knowledge.

The development of the flight load estimators – the "*virtual loads sensors*" – for a load station at the HTP are presented. The vital choice of sensitive parameters to obtain the mapping function is explained. A new optimised splitting algorithm further improves the modelling in the case that subspaces contain only few data samples.

The models developed to estimate loads like bending and torsional moments and shear forces generalise well on both: data from design calculations and flight test data. The models developed exceed rarely an error margin of 10% limit load but never exceed 20% in general. The models are especially trimmed towards high loads where the error margin is always below 10% limit load.

Further studies, like the application of this concept to other structural parts of an aircraft, namely fuselage and wing have been investigated in [5]. Open topics are transition phases like flight-ground transitions and the use of electronic flight control systems and high-lift systems. The method could also be combined with other, for example observer based methods.

Copyright Statement

References

[1] Transportation Safety Board of Canada (TSB), "Aviation Investigation Report, Loss of Rudder in Flight Air Transat, Report Number A05F0047," Tech. rep., Minister of Public Works and Government Services Canada, 2007.

[2] Aerospace Industries Association, "Best Practices Guide, Inspection Processes following High Load Events," April 2005.

[3] Halle, M., Thielecke, F., and Lindenau, O., "Comparison of real-time flight loads estimation methods," *CEAS Aeronautical Journal*, Vol. 5, No. 4, 2014, pp. 501–513.

[4] Halle, M. and Thielecke, F., "Flight Loads Estimation Using Local Model Networks," *29th Concress of the International Council of the Aeronautical Sciences, St. Petersburg 07. - 12. Sept. 2014*, International Council of the Aeronautical Sciences (ICAS), September 2014.

[5] Halle, M., "Lokalmodell-Netz-Identifikation als Analyse- und Bewertungsmethodik von Flugmanöverlasten," Dissertation, Shaker Verlag, 2016.

[6] Skopinski, T. H., Aiken, W. S., and Huston, W. B., *Calibration of strain-gage installations in aircraft structures for the measurement of flight loads*, Vol. 1178 of *Report / National Advisory Committee for Aeronautics*, US Gov. Print. Off, Washington and DC, 1954.

[7] Brökelmann, M., "Dehnungsmessung mit Faser-Bragg-Gitter am Holmgurt der SB14 der Akaflieg Braunschweig im Flugversuch," Tech. rep., Akademische Fliegergruppe (Akaflieg) Brauschweig e.V., 2003.

[8] Schroeder, K., Ecke, W., Apitz, J., Lembke, E., and Lenschow, G., "A fibre Bragg grating sensor system monitors operational load in a wind turbine rotor blade," *Measurement Science and Technology*, Vol. 17, Institute of Physics Publishing, 2006, pp. 1167–1172.

[9] Qing, X. P., Yuan, S., and Wu, Z., "Current Aerospace Applications of Structural Health Monitoring in China," *6th European Workshop on Structural Health Monitoring*, 2012.

[10] Kim, D. and Pechaud, L., "Improved methodology for the prediction of the empennage maneuver in-flight loads of a general aviation aircraft using neural networks," Tech. rep., Federal Aviation Agency, FAA, 2001.

[11] Allen, M. J. and Dibley, R. P., "Modeling aircraft wing loads from flight data using neural networks," Tech. rep., NASA Dryden Flight Research Center, 2003.

[12] Allen, M. J., Lizotte, A. M., Dibley, R. P., and Clarke, R., "Loads Model Development and Analysis for the F/A-18 Active Aeroelastic Wing Airplane," Tech. rep., NASA Dryden Flight Research Center, 2005.

[13] Reed, S., "Indirect aircraft structural monitoring using artificial neural networks," *The Aeronautical Journal*, Vol. 112, No. 1131, May 2008, pp. 251–265.

[14] Reed, S., McCoubrey, B., and Mountfort, A., "Introduction to Service of an Artificial Neural Network Based Fatigue Monitoring System," *25th Symposium of the International Committee on Aeronautical Fatigue, Rotterdam, The Netherlands*, 2009.

[15] Fuentes, R., Cross, E., Halfpenny, A., Worden, K., and Barthorpe, R. J., "Aircraft Parametric Structural Load Monitoring Using Gaussian Process Regression," *7th European Workshop on Structural Health Monitoring*, 2014.

[16] Murray-Smith, R., "Local Model Networks and Local Learning," *Fuzzy Duisburg*, 1994, pp. 404–409.

[17] Nelles, O., *Nonlinear System Identification*, Springer-Verlag Berlin, Heidelberg, New York, 2001.

[18] Bänfer, O. and Nelles, O., Kainz, J. and Beer, J., "Local Model Networks with Modified Parabolic Membership Functions," *International Conference on Artificial Intelligence and Computational Intelligence*, 2009.

[19] Bänfer, O. and Nelles, O., "Polynomial Model Tree (POLYMOT) - A New Training Algorithm for Local Model Networks with Higher Degree Polynomials," *IEEE International Conference on Control and Automation*, 2009.

[20] Giesemann, P., *Identifizierung nichtlinearer statischer und dynamischer Systeme mit Lokalmodell-Netzen*, Ph.D. thesis, TU Braunschweig, Institut f. Flugsystemtechnik, 2002.

[21] Nelles, O., "Axes-Oblique Partitioning Strategies for Local Model Networks," *Proceedings of the IEEE International Symposium on Intelligent Control*, 2006.

[22] Wright, J. R. and Cooper, J. E., *Introduction to Aircraft Aeroelasticity and Loads*, John Wiley & Sons, Ltd., 2007.

[23] Britxe, D. and Traverse, P., "AIRBUS A320/A330/A340 Electrical Flight Controls – A Family of Fault-Tolerant Systems," *The Twenty-Third International Symposium on Fault-Tolerant Computing, FTCS-23*, 1993, pp. 616 – 623.